Proceedings of ITC18, 2008

Collective Thomson Scattering Study using Gyrotron in LHD

Shin KUBO[1)], Maski NISHIURA[1)], Kenji TANAKA[1)], Takashi SHIMOZUMA[1)], Yoshinori TATEMATSU[2)], Takashi NOTAKE[2)], Teruo SAITO[2)], Yasuo YOSHIMURA[1)], Hiroe IGAMI[1)], Hiromi TAKAHASHI[1)], Namiko TAMURA[3)]

[1)]*National Institute for Fusion Science,322-6 Oroshi-cho, Toki 509-5292, Japan*
[2)]*Research Center for Development of FIR Region, Univ. of Fukui, Fukui, 910-8507, Japan*
[3)]*Dept. of Energy Science and Technology, Nagoya Univ., Nagoya, 464-8463, Japan*

The collective Thomson scattering (CTS) is one of the most promising methods for evaluating the ion velocity distribution function. The study of CTS diagnostic has been started utilizing the gyrotron and antenna/transmission systems installed in LHD for high power local electron heating. One of the high power gyrotrons at 77 GHz is selected as a probing power source and a set of highly focused antenna system is used for the probing and receiving antenna. The specific feature of the system, receiver design are described and preliminary data obtained in for ECRH plasma in LHD are discussed.

Keywords: Collective Thomson scattering, ECRH, ECE, Gyrotron, Gaussian beam, Ion temperature

1 Introduction

The direct and local measurement of the ion velocity distribution function is important in any fusion relevant plasma to study the behaviors of not only the bulk but also the high energy ions. The collective Thomson scattering (CTS) has long been attracted and intensively studied as one of the most promising diagnostic methods for the ion distribution function[1]. Frequency range required for the CTS in the fusion relevant plasma is determined from the collective scattering condition and scattering angle that gives the spatial resolution. This frequency range lies from infrared to millimeter wave[2, 3, 4]. Mainly due to a small scattering cross section, or scattering efficiency, CTS requires high power probe beam source with sharp single frequency spectrum and highly sensitive receiver near the frequency but avoiding a direct contamination of the probe frequency that requires a sophisticated stray suppression. The other important factor required for the spatially well resolved measurement of CTS is the well defined probe and receiving beams and their controllability. High power, sharp spectrum, and highly focussed well defined Gaussian beam are already realized for the electron cyclotron resonance heating (ECRH) system using gyrotron and high power transmission/antenna in LHD. We have started the trial of CTS study utilizing the existing ECRH system in LHD[5] as well as that utilizing higher frequency (400 GHz) gyrotron that is under development[6]. Expected necessary frequency range to deduce ion velocity distribution is ± 3 GHz at the center frequency. In section 2 are discussed the characteristic feature of the ECRH system in LHD as a CTS probe and receive beam. Electron cyclotron emission (ECE) is expected to be the main source of noise for CTS diagnostic. The ECE spectrum expected at the line of receiving beam is discussed in section 3. Receiver system is described in section 4. Finally the preliminary data obtained with the system described here are shown in section 5.

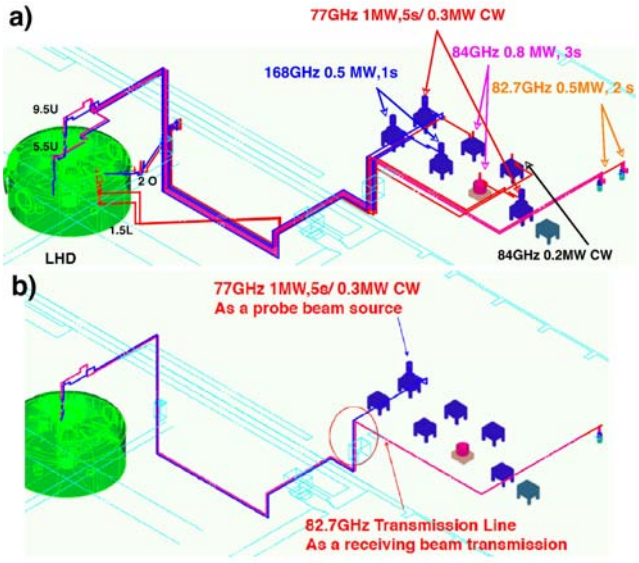

Fig. 1 a) Two sets of injection antenna system are installed on 4-ports of LHD, (5.5U, 9.5 U, 1.5L and 2O). b) A set of transmission line/ antenna on the 9.5U port is selected for CTS. The set that 77GHz 1MW power is available is used for probe beam.

2 ECRH system as a probe beam and receiver antenna for CTS

One of the newly installed 77 GHz gyrotrons in LHD have achieved more than 1MW over 3 s[7]. The present ECRH system is illustrated in Fig. 1 a). Nine gyrotrons are in operational and eight corrugated transmission lines (6- 88.9

author's e-mail: kubo@LHD.nifs.ac.jp

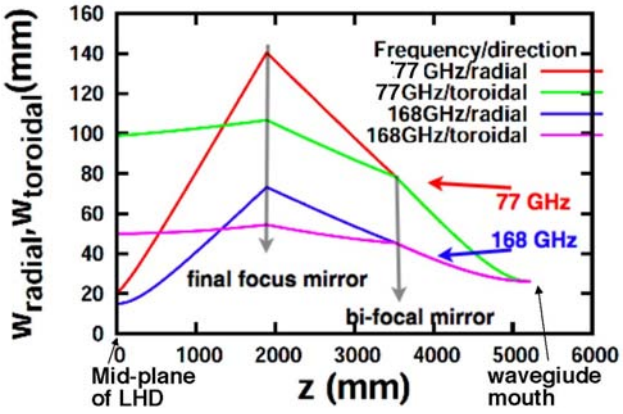

Fig. 2 Beam evolution at 9.5 U port antenna. Originally the focusing mirrors are originally optimized for 168 GHz to focus the symmetric Gaussian beam radiated from 88.9 mm corrugated waveguide to an elliptical Gaussian beam on the mid-plane of LHD to have *1/e* waist size of 15 mm and 50 mm in radial and toroidal direction, respectively. Re-calculated beam evolutions for 77 GHz are plotted. The waist size for 77 GHz are also elliptical Gaussian with the waist size on the LHD-midplane 20 and 100 mm.

id and 2-31.75 mm id) are connected to LHD. Two sets of injection antenna are installed on each 4-LHD ports (5.5U, 9.5U, 2-O and 1.5L). The 9.5 U port antenna set is selected as a CTS probe and receiving antenna, since 77 GHz high power is available for the probing beam and the beam controllability is well established and confirmed [8]. This gyrotron has a triode gun that allows high frequency power modulation without degrading oscillating mode which is one of the important feature for the CTS. This gyrotron is connected to one of the Gaussian mirror antenna set. This antenna set includes one another Gaussian beam mirror suitable for receiving the scattered power from definite scattering volume. The injection antenna used was originally designed for 168 GHz. The beam evolutions for 77 GHz is re-calculated using the same mirror sets and configurations as 168 GHz, using the mirror curvature and phase plane transformation relation:

$$\frac{\cos\phi}{\rho_\sigma} = \frac{1}{2R_{\sigma,\mathrm{in}}} + \frac{1}{2R_{\sigma,\mathrm{out}}} \tag{1}$$

here, ϕ is the injection/reflection angle, $R_{\sigma,\mathrm{in}}$, $R_{\sigma,\mathrm{out}}$ and ρ_σ are the phase radius of input and output beams and mirror curvature radius in σ =toroidal or poloidal directions. Actual beam configuration is shown in Fig. 3 for the case where the center of the scattering volume lies near $\rho \approx 0.7$. The upper half of the flux surfaces of $\rho = 0.1$ and 1.0 are also shown for reference. The effective scattering volume can be calculated by integrating over the space using the

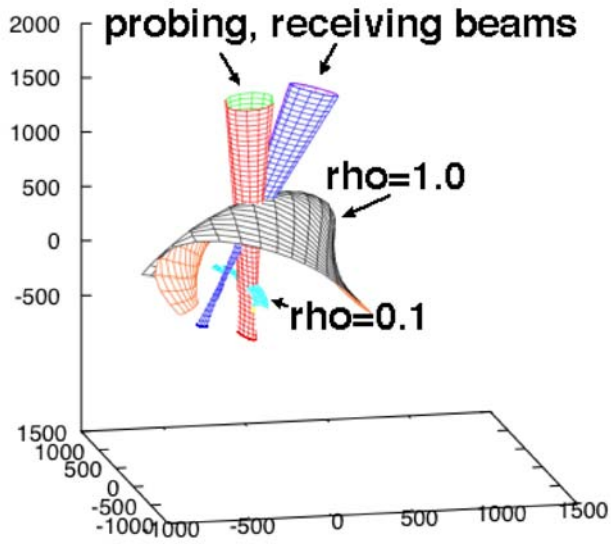

Fig. 3 3-D image of the probe and receiving beams.

following formula

$$\iint \exp\left(-\frac{x^2}{w_{0,\mathrm{x}}^2+\frac{\lambda^2(z-z_{0,\mathrm{x}})^2}{\pi^2 w_{0,\mathrm{x}}^2}} - \frac{y^2}{w_{0,\mathrm{y}}^2+\frac{\lambda^2(z-z_{0,\mathrm{y}})^2}{\pi^2 w_{0,\mathrm{y}}^2}}\right) \exp\left(-\frac{x'^2}{w_{0,\mathrm{x}'}^2+\frac{\lambda^2(z'-z_{0,\mathrm{x}'})^2}{\pi^2 w_{0,\mathrm{x}'}^2}} - \frac{y'^2}{w_{0,\mathrm{y}'}^2+\frac{\lambda^2(z'-z_{0,\mathrm{y}'})^2}{\pi^2 w_{0,\mathrm{y}'}^2}}\right) \delta(\boldsymbol{r}' - \overleftrightarrow{\boldsymbol{T}} \cdot \boldsymbol{r})\mathrm{d}\boldsymbol{r}\mathrm{d}\boldsymbol{r}'. \tag{2}$$

Here, λ is the wavelength, $w_{0,\sigma}$, $z_{0,\sigma}$ are the waist size and waist position in $\sigma = x, y, x', y'$. (x, y, z) is the local coordinate of injection beam and (x', y', z') is that of receiving beam and $\overleftrightarrow{\boldsymbol{T}}$ is the conversion tensor of both local coordinates. The scattering volume for the case shown in Fig. 3 is about 700 cm^3. This volume is distributed over the minor radius 0.78 ± 0.2 as shown in Fig. 4. This figure defines the spatial resolution of the CTS measurement using this antenna set.

3 Background ECE as a main noise source

Main competing background noise source for CTS is the electron cyclotron emission (ECE). The background ECE level on the line of sight toward the receiver antenna should be estimated taking account of the actual antenna configuration. The calculation of the background ECE spectrum is performed by solving the radiation transfer equation back along the line of sight. The method is described in ref[9]. For use of this 77 GHz gyrotron as a probing beam, operational magnetic field should be selected so as to exclude the fundamental and second harmonic resonances of 77 GHz on the line of sight inside the plasma confinement region, in order to reduce the ECE background that is considered to be the largest noise source. The relations be-

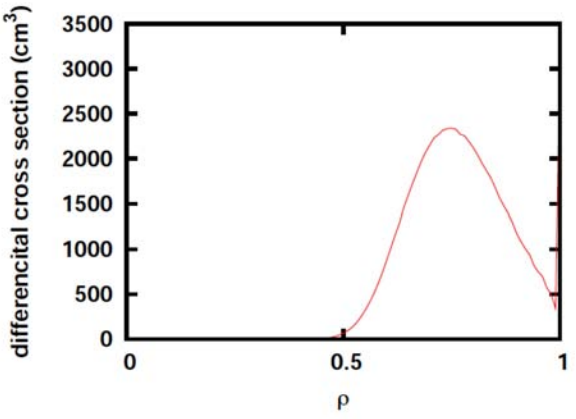

Fig. 4 Differential cross section of the scattering volume as a function of effective minor radius ρ. The scattering volume center is placed at z=0.5 m, R=3.6 m on the vertically elongated poloidal cross section in LHD. Total effective scattering volume is about 700 cm^3 in this case.

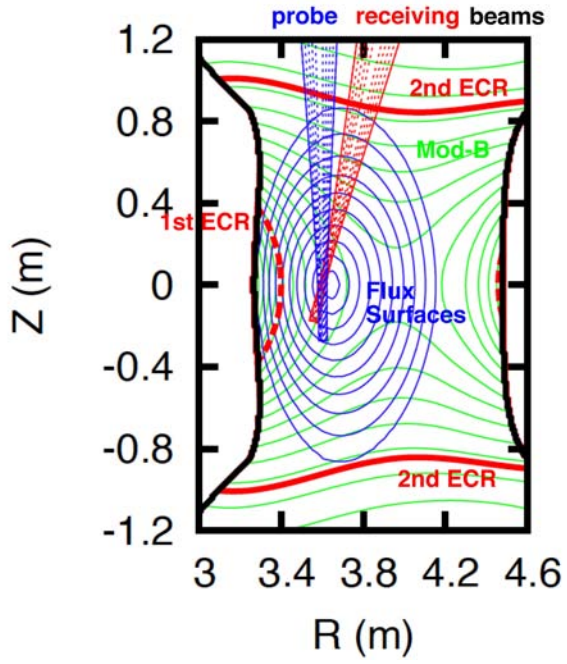

Fig. 5 Relation between probing, receiving beams, flux surfaces and EC resonances for the case of magnetic field setting B_0=2.2 Tesla on the vertically elongated cross section in LHD.

tween resonances and probing, receiving beam on the vertically elongated cross section in LHD are shown in Fig. 5. Setting higher magnetic field would place the fundamental resonance layer inner to the higher electron temperature region, causing higher background ECE level taking into account of the multi-reflection. On the other hand, setting lower magnetic field would place the second harmonic resonance layer on the receiving line of sight. In Figure 6 are shown the calculated O and X mode ECE spectrum for the cases of central electron temperature $T_{e,0}$= 5 keV and 1 keV. By setting the magnetic field near 2.2 Tesla, one can expect the background ECE level minimum, although the multi-reflection effect can increase the contribution from fundamental resonance. Due to its complexity of magnetic field structure in LHD, there exists fundamental and second harmonic resonance simultaneously in any settings of magnetic field strength. In such configurations, some adjustment of setting magnetic field would necessary to minimize the ECE background and at the same time to avoid the absorption of scattered power.

4 Receiver system for CTS

A receiver system is installed on the upstream of the transmission line, which is normally used for high power transmission line for ECRH. A waveguide switch is attached on the 88.9 mm id corrugated waveguide transmission system at the marked position in Fig. 1 b). A heterodyne receiver is placed at the output of the waveguide switch. The receiver consists of a high sensitive heterodyne radiometer. The circuit diagram is shown in Fig. 7 a).

At the front end, two multi-stage notch filters with the 3 dB band width of 300 MHz and attenuation -120 dB at the center frequency, 76.95 GHz, are placed to avoid the high level stray radiation that can damage the mixer or make ghost signal at the mixer and make saturation of the intermediate frequency (IF) amplifier. A pin-switch is also inserted to block the spurious mode which might be excited at the turn on or off of the gyrotron out of the notched but sensitive frequency. Band pass filter from 72 to 82 GHz to filter out the lower side band of the mixer of the local frequency at 74 GHz is also placed in front of the mixer. Intermediate frequency from 300 MHz to 10 GHz at the upper side band of the mixer is amplified by low noise amplifier and splitted to filter bank. Since the gyrotron oscillating frequency can subject to the shift of the order of 100 MHz during the oscillation or at the ramping up phase

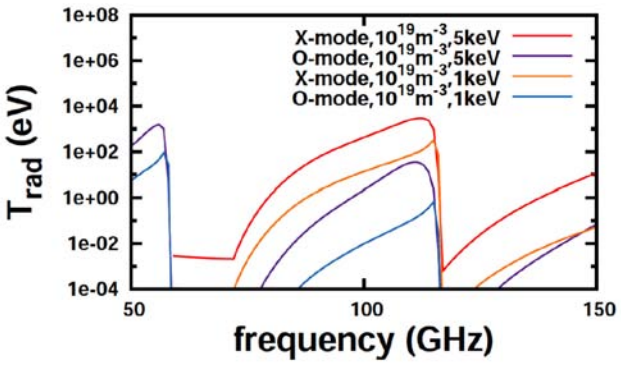

Fig. 6 Calculated ECE spectrum for the line of sight of CTS receiving antenna. Electron temperature is assumed to have $T_{e,0}(1-\rho^2)^2$. Here the magnetic field is set B=2.2 Tesla.

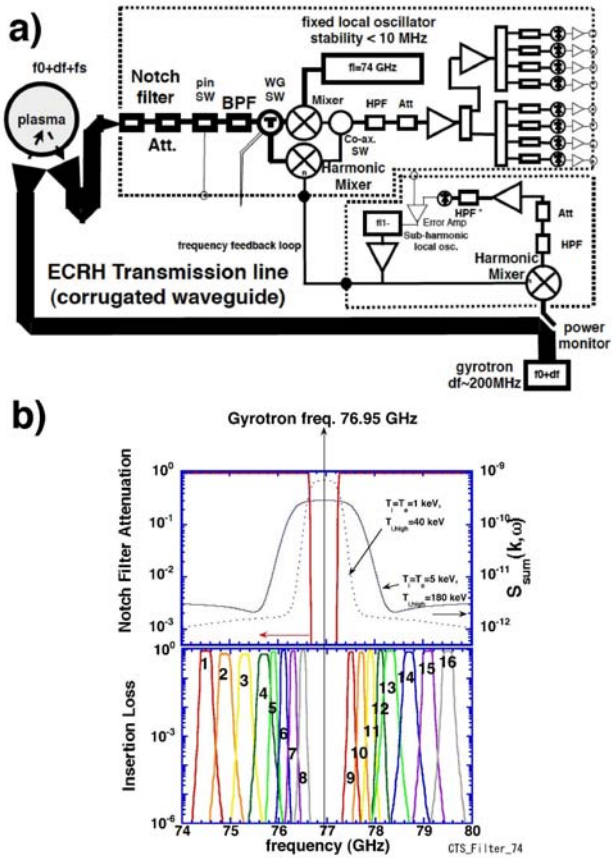

Fig. 7 a) Block diagram of the heterodyne receiver for CTS in LHD. The notch filter, band pass filter and pin-switch are placed in front of the mixer. Fixed local frequency at 74 GHz is normally used. b)Characteristics of the filter prepared for the local frequency at 74 GHz expected from the characteristic curve at the IF. Expected notch filter response with calculated CTS spectrum are shown in the upper column.

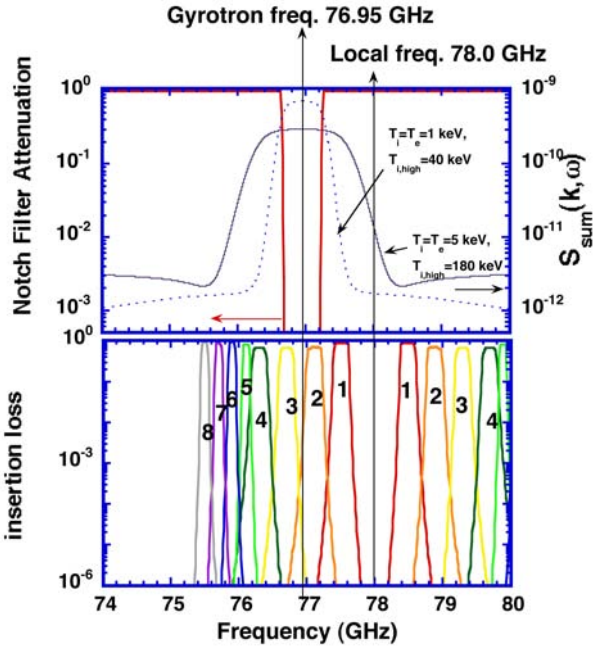

Fig. 8 Characteristics of the filter prepared for the local frequency at 78 GHz expected from the characteristic curve at the IF. Expected notch filter response is shown above.

of the anode voltage, IF center frequency tracking system using harmonic mixer will be also attached for the precise estimation of the bulk component. Filter bank consists of 8 to 16 filters at the first trial. Fig. 7 b) are shown the expected response of the notch and bank filters in the upper and lower column, respectively. Here, calculated CTS spectrum for the cases where the bulk ion and electron temperatures are 1 keV with high enegy ions of 40 keV and 5 keV with 180 keV high energy ions are over plotted in the upper column.

5 Preliminary Results

At the adjustment phase of the CTS receiver system, the local oscillator was damaged and the Gunn oscillator at 78 GHz is used in stead of 74 GHz. With this local frequency, expected frequency response of the receiver is shifted as shown in Fig. 8. In this case, channel 1 to 4 becomes sensitive at both upper and lower side bands of the local frequency. As is expected from the calculated CTS spectrum, channel 1 to 4 are sensitive to the bulk ion temperature and channel 5 to 8 are more sensitive to high energy ion components. Preliminary signals were obtained from the ECRH plasma without NBI at the magnetic field of 2.75 Tesla. Electron density levels was 1×10^{19} m^{-3}. Plasma parameters are kept only by the 77 GHz ECRH which is also used as a probing beam. Nominal electron temperature was 3 keV at the center. The injected power is 100% modulated at the frequency of 50 Hz from 0.25 to 1.15 s, 1.25 to 1.75 s and 1.85 s to 2.25 s. In Fig. 9 are shown detected signals at each filer channel from 1 to 8 indicated in Fig. 8. Raw signals contain sharp spikes at each modulation that may be attributed to the spurious mode oscillation from the gyrotron. These spikes are almost subtracted but failed from 1.3 to 1.6 s in this figure. The signals during on and off phases are separated and displayed by red and green lines. It seems that the background ECE level and scattered signal level are well separated at channels 1 to 4 and barely at channel 5 and 6. Shown in Fig. 10 are the expanded signals in time from 1.0 to 1.1 s. These signals show clear characteristics of the scattering signals in contrast to the change of the ECE background which is small and should be continuous. Although several checks are to be done, these signals show expected feature of the scattering signals. The sensitivity calibration of each channels are underway. The deduction of the CTS spectrum from these data would be possible after this calibration.

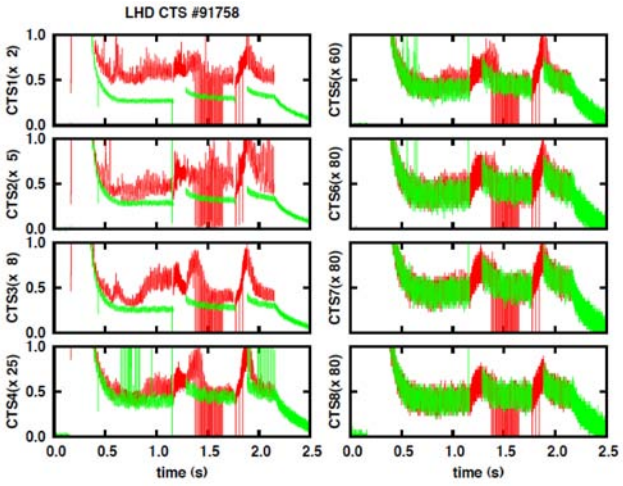

Fig. 9 Preliminary data from each filter bank channel as indicated in Fig. 8. Detected signals are separated by on and off phase of the probing beam and indicated by red and green lines.

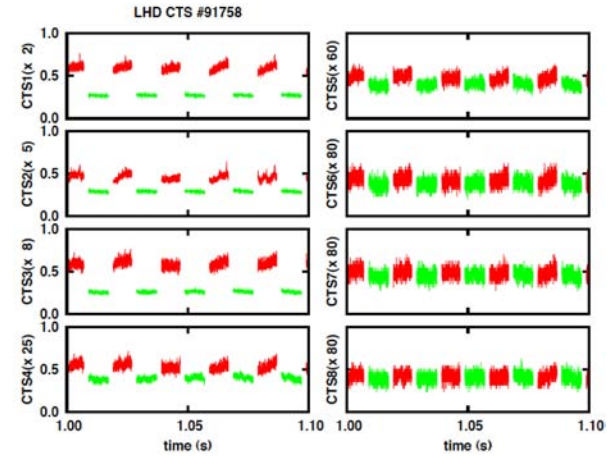

Fig. 10 Expanded figure in time from 1.0 to 1.1 s of Fig. 9. The increase of the ECE background can well be separated from the step-wise increase/ decrease at turn-on and -off time especially in channels 1 to 6.

Summary

The CTS system is conformed utilizing the characteristic features of the LHD ECRH system. These features includes well controlled and strongly focused Gaussian beam antenna, high power low loss transmission lines. From the expected Gaussian beam, the method of estimating the beam cross section is established and shown the spatial resolution of CTS measurement. CTS receiver is designed and constructed to detect the scattering signals in the range of ± 3 GHz at 77 GHz. Preliminary signals are obtained for ECRH plasma at the density of 1×10^{19} m^{-3}. Furthermore check and calibration is necessary to confirm and deduce ion velocity distribution function from these data.

[1] H. Bindslev, S. K. Nielsen, L. Porte, J. A. Hoekzema, S. B. Korsholm, F. Meo, P. K. Michelsen, S. Michelsen, J. W. Oosterbeek, E. L. Tsakadze, E. Westerhof, and P. Woskov, Phys. Rev. Lett. **97**, 205005 (2006).

[2] T. Kondoh, S. Lee, D. P. Huchinson and R. K. Richards, Review of Scientific Instruments **72**, 1143 (2001).

[3] S. Michelsen, S. B. Korsholm, H. Bindslev, F. Meo, P. K. Michelsen, E. L. Tsakadze, J. Egedal, P. Woskov, J. A. Hoekzema, F. Leuterer and E. Westerhof, Review of Scientific Instruments **75**, 3634 (2004).

[4] F. Meo, H. Bindslev, S. B. Kolsholm, E. L. Tsakadze, C. I. Walker, P. Woskov G. Vayakis, Review of Scientific Instruments **75**, 3585 (2004).

[5] M. Nishiura, K. Tanaka, S. Kubo, T. Saito, Y. Tatematsu, T. Notake, K. Kawahata, T. Shimozuma, T. Mutoh, Review of Scientific Instruments **79**, 10E731 (2008).

[6] T. Notake, T. Saito, Y. Tatematsu, S. Kubo, T. Shimozuma, K. Tanaka, M. Nishiura, A. Fujii, La Agusu, I. Ogawa, T. Idehara, Rev. Sci. Instrum. **79**, 10E732 (2008).

[7] H. Takahashi, T. Shimozuma, S. Kubo, S. Ito, S. Kobayashi, Y. Yoshimura, H. Igami, Y. Mizuno, Y. Takita, T. Mutoh, T. Kariya, R. Minami, T. Imai, Submitted to Fusion Science and Technology.

[8] S. Kubo, T. Shimozuma, Y. Yoshimura, H. Igami, H. Takahashi, *et al.*, Proc. 22nd IAEA Fusion Energy Conference, 13-18 October 2008 Geneva, Switzerland. EX/P6-14.

[9] S. Kubo, H. Igami, Y. Nagayama, S. Muto, T. Shimozuma, Y. Yoshimura, H. Takahashi and T. Notake, Proc. of International Congress on Plasma Physics 2008, 8-12 September 2008, Fukuoka Japan; Submitted to Plasma and Fusion Research.